INSTITUTE OF PHYSICS PUBLISHING JOURNAL OF PHYSICS B: ATOMIC, MOLECULAR AND OPTICAL PHYSICS

J. Phys. B: At. Mol. Opt. Phys. **39** (2006) 4289–4299 doi:10.1088/0953-4075/39/20/025

Electron collision with $B(CD_3)_3$ molecules

Alicja Domaracka, Paweł Możejko, Elżbieta Ptasińska-Denga and Czesław Szmytkowski

Atomic Physics Group, Department of Atomic Physics and Luminescence, Faculty of Applied Physics and Mathematics, Gdańsk University of Technology, ul. Gabriela Narutowicza 11/12, 80-952 Gdańsk, Poland

E-mail: czsz@mif.pg.gda.pl

Received 5 July 2006, in final form 13 August 2006
Published 10 October 2006
Online at stacks.iop.org/JPhysB/39/4289

Abstract

Absolute total cross section (TCS) for electron–trimethylborane-d_9 ($B(CD_3)_3$, TMB-d_9) collisions has been measured at energies ranging from 0.4 to 370 eV using the linear electron-transmission technique. The most visible feature of the TCS energy function is a pronounced broad enhancement peaked between 5 and 10 eV. Some weak structures are also perceptible in the TCS curve. At intermediate energies the experimental results are compared with the cross section obtained as a sum of the integral elastic and ionization cross sections calculated in this work for the $B(CH_3)_3$ molecule. Similarities observed in cross sections for planar, boron-containing BX_3 (X = F, Cl, CD_3) molecules are also pointed out and discussed.

(Some figures in this article are in colour only in the electronic version)

1. Introduction

Electron-assisted processes play an important role in a wide range of industrial and environmental applications; they are also of scientific interest (see [1, 2] and references therein). For understanding and modelling reactions involved in plasma-enhanced technologies, effects of ionizing radiation in living cells, and/or processes in interstellar media, knowledge of comprehensive sets of electron-scattering data is invaluable. Unfortunately, in spite of great experimental and theoretical effort, most data sets for compounds of current scientific and technological interest, especially those in absolute scale, are rather sparse. The reason for the deficiency of reliable electron-scattering data lies partly in experimental as well as in computational difficulties. Some help in the estimation of the required data which are difficult to obtain may come from regularities found in cross sections which are already known for other targets or from computations based on approximate methods. Some regularities in total cross section (TCS) energy dependence we have already noted for selected target families (cf [3, 4]). The observed effects shed a new light on the role of molecular target constituents

(e.g. *perfluorination effect* [3]) in the electron scattering as well as onto the role of atom arrangement in the molecule (*isomeric effect* [4]). Up to now, however, attention in the above-mentioned experiments has been paid mainly to hydrocarbons and their perfluorinated equivalents. To find out if any regularities in TCS energy functions can be observed also for other groups of targets, we have recently focused on the family of symmetric planar, and non-polar, boron-containing molecules.

The present work has several goals: first, to provide the electron-scattering absolute TCS for trimethylborane-d_9 (TMB-d_9, $B(CD_3)_3$) over a wide electron-impact energy range, from low to intermediate; second, to explore some trends in the TCS of boron-containing molecules (BF_3 [5], BCl_3 [6], $B(CD_3)_3$) to look for possible regularities in the TCS energy curve behaviour; and third, to compute cross sections for the electron–molecule scattering at energies beyond the range of experiments.

Studies on the electron-assisted processes involving trimethylborane (TMB) molecules started some decades ago; however, the data still remain scarce and fragmentary. At first, the electrons were used as projectiles to obtain the diffraction pattern [7, 8] from which the molecular structure of TMB was established. Later, experiments concerned mainly the investigation of electron-induced formation of positive [9–14] and negative ions [13]. These studies provided information on appearance potentials only and/or gave relative abundances of the observed ions. To our knowledge no absolute intensities, neither measured nor calculated, have yet been reported for electron scattering by the trimethylborane-d_9 molecule or its perhydrogenated counterpart.

Trimethylborane was at first used in proportional neutron counters [15]. Nowadays, TMB or TMB-d_9 are used as doping sources of boron in manufacturing of diamond [16] and/or silicon films [17] for optoelectronic devices.

2. Methods and procedures

2.1. Experimental details

The absolute total electron-scattering cross section for the TMB-d_9 molecule has been measured employing the electron transmission method in a linear configuration under single collision conditions [18]. Detailed description of the experimental set-up and procedures has been already given in earlier reports (e.g. [19]), therefore only a short summary will be presented here. In brief, the electron beam with an energy spread of about 0.1 eV (FWHM) is generated by a filament and an electron optics set composed of an electron gun followed by a 127° cylindrical electrostatic energy dispersing condenser and a zoom lens system. The electrons of a given energy, E, are directed into a scattering cell. Those getting away from the reaction volume through the exit slit are energy-discriminated by a retarding-field analyser to avoid detection of inelastically scattered electrons, and eventually they are collected by a Faraday cup detector. The magnetic field in the electron optics volume is reduced to the value below 0.1 μT. The electron energy scale is calibrated based on the well-known resonant oscillatory structure in N_2 observed in the vicinity of 2.3 eV (e.g. [20]).

With a target let into the reaction cell, the electrons suffer scattering that is reflected in the attenuation of the recorded transmitted electron current. Based on the Bouguer–de Beer–Lambert (BBL) relationship

$$Q(E) = \frac{1}{nl} \ln \frac{I(E, 0)}{I(E, p)},$$

the value of the total cross section, $Q(E)$, can be derived from the intensities of the transmitted electron currents taken in the presence, $I(E, p)$, and absence, $I(E, p = 0)$, of the target in

the cell. The other quantities used in the BBL formula are n—the absolute number density of target molecules in the collision volume, and l—the length of the electron pathway within the target.

Introductory measurements revealed that trace amounts of the investigated gas, TMB-d_9, effusing from the reaction cell through the entrance and exit orifices into the volume of the electron optics, influence the filament emission and to some extent also the transmission of electrons through the spectrometer. These effects increase with the time the electron optics are subjected to the sample gas and may markedly distort the measured electron currents and, in consequence, may affect the measured TCS. To lessen such effects, the first step of the experiment involved prolonged passivation of the electron optics by $B(CD_3)_3$. Prior to the TCS measurements, the vacuum chamber (with the electron optics) was filled up for a period of about 2 days with the target vapour at an elevated pressure of about 1 mPa and a temperature of 325 K. Such treatment provided a nearly stable electron current during a 1 month experiment. Moreover, to ensure that conditions in the region of electron optics are almost invariable throughout the experiment, irrespective of whether the target was present or absent in the collision cell, the gas sample was supplied alternately into the cell or in its surrounding.

The final TCS value at given energy of impinging electrons is a weighted mean of results from 4–8 series, each containing 7 to 10 individual runs. The particular runs have been carried out at slightly different electron-optics operating voltages and over the range of the sample pressure in the scattering cell (40–80 mPa); the working pressure in the vacuum chamber is then well below 0.2 mPa. With the use of the aforementioned procedure, the TCS values obtained in series for a particular energy appeared to be independent, within the limits of random scatter, of the applied incident electron current (0.2–10 pA) and the target gas pressure, over a long duration of the experiment. The statistical scatter of measurements was sufficiently low to reveal weak TCS structures; they were discernible in each series of runs. The statistical uncertainty (one standard deviation of the weighted mean value) of the measured absolute TCS results is well below 1% over the whole investigated energy range.

The overall systematic uncertainty in the measured TCS is about 6% below 2 eV, decreasing gradually to 4–5% between 6 and 100 eV, and increasing to 6–8% at higher energies. Major potential sources of systematic error in the present TCS measurements are related to the uncertainty in the determination of the factor nl in the attenuation BBL formula and to incomplete discrimination against electrons scattered at small forward angles. Due to inevitable effusion of the target particles across orifices, through which electrons enter and leave the reaction cell, neither the density number of the target (n) along the electron pathway nor the distance (l) within which electrons suffer the scattering with the target can be precisely determined. In the present experiment, the denominator nl is estimated as the product of the target density number, $n = p/k\sqrt{T_m T_t}$, derived from the ideal gas law using the absolute measurements of the gas target pressure, p, in the centre of the cell, and the temperatures of the target, T_t and the mks manometer head, T_m (the thermal transpiration effect has been taken into account [21]), while l is assumed to be equal to the geometrical distance between orifices of the scattering cell, L (=30.5 mm). Calculations, based on [22], show that in the present experimental conditions such approach effects in the TCS error of 3–4%. Incomplete discrimination against electrons which have undergone scattering in small-angle forward directions tends to lower the TCS measured in the electron-transmission experiments. This is due to finite angular resolution of the used detector system (about 0.8 msr in the present geometry) and to the inability to discriminate electrons with kinetic energies that differ from the impact energies by no more than tenths of an eV. The uncertainty in the TCS, related to this effect, usually increases with impact energy and with electric dipole moment

of the target molecule. Estimations, based on our elastic differential cross sections (DCS) calculated at intermediate energies, indicate that the TCS lowering due to forward scattering should not exceed 2–3% at the highest applied energies. Due to lack of low-energy DCSs, the uncertainty below 50 eV may be only roughly estimated on the basis of data for other non-polar molecules ($\mu = 0$ for $B(CD_3)_3$ in its ground state) of similar size; that gives values of about 1–2% in the low-energy range. The comprehensive analysis of particular components of the systematic uncertainty has been already discussed elsewhere [23].

A commercially supplied sample of $B(CD_3)_3$ with a purity of 99% (as stated by Aldrich) was used directly from the container without further purification and no analysis of the gas was made.

2.2. Computational

Theoretical approaches and computational procedures employed in the present work for obtaining intermediate-energy electron–molecule scattering cross sections have been described previously [5, 24, 25], so only the key points will be briefly outlined in this section. To investigate the problem of elastic electron collisions with studied molecules the independent atom method (IAM) [26] has been used. In that method the problem of electron–molecule scattering is reduced to electron scattering by atoms constituting the molecule, under the following assumptions: (i) each atom of the molecule scatters independently, (ii) redistribution of atomic electrons due to molecular binding is unimportant, and (iii) multiple scattering within the molecule is negligible [26]. Thus, this approach is valid and can provide reasonable results for intermediate- and high-collision energies only (e.g. [24, 27] and references therein).

The integral elastic electron–molecule scattering cross section (ECS) within the IAM method is given by

$$\sigma_{\mathrm{el}}(E) = \frac{4\pi}{k} \sum_{i=1}^{N} \mathrm{Im}\, f_i(\theta = 0, k) = \sum_{i=1}^{N} \sigma_i^{\mathrm{A}}(E), \tag{1}$$

where E is an energy of the incident electron, $f_i(\theta, k)$ is the scattering amplitude due to the ith atom of the molecule, θ is the scattering angle, and $k = \sqrt{2E}$ is the wave number of the incident electron. The atomic elastic cross section for the ith atom of the target molecule, $\sigma_i^{\mathrm{A}}(E)$, has been computed according to

$$\sigma^{\mathrm{A}} = \frac{4\pi}{k^2} \left(\sum_{l=0}^{l_{\max}} (2l+1) \sin^2 \delta_l + \sum_{l=l_{\max}}^{\infty} (2l+1) \sin^2 \delta_l^{(\mathrm{B})} \right). \tag{2}$$

To obtain phase shifts, δ_l, partial wave analysis has been employed and the radial Schrödinger equation

$$\left[\frac{\mathrm{d}^2}{\mathrm{d}r^2} - \frac{l(l+1)}{r^2} - 2(V_{\mathrm{stat}}(r) + V_{\mathrm{polar}}(r)) + k^2 \right] u_l(r) = 0, \tag{3}$$

has been solved numerically under the boundary conditions

$$u_l(0) = 0, \qquad u_l(r) \overset{r\to\infty}{\longrightarrow} A_l \hat{j}_l(kr) - B_l \hat{n}_l(kr), \tag{4}$$

where $\hat{j}_l(kr)$ and $\hat{n}_l(kr)$ are the Riccati–Bessel and Riccati–Neumann functions, respectively. The electron-atom interaction has been represented by static, $V_{\mathrm{stat}}(r)$, [28] and polarization, $V_{\mathrm{polar}}(r)$, [29] potentials.

In the present calculations the exact phase shifts, δ_l, have been calculated up to $l_{\max} = 50$, while those remaining, $\delta_l^{(\mathrm{B})}$, have been included through the Born approximation.

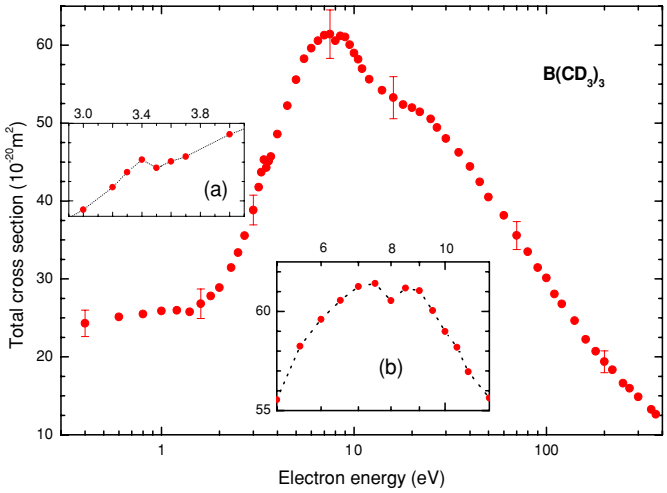

Figure 1. Present experimental absolute total cross section (TCS) for e^-–$B(CD_3)_3$ scattering (●); error bars represent overall (systematic plus statistical) uncertainties. Insets highlight the TCS features: (a) the 3.4 eV peak; (b) the two-peaked maximum; lines are added to guide the eye.

Electron-impact ionization cross sections have been obtained within the binary-encounter-Bethe (BEB) formalism [30]. Within this formalism the electron-impact ionization cross section per molecular orbital is given by

$$\sigma^{\mathrm{BEB}} = \frac{S}{t+u+1}\left[\frac{\ln t}{2}\left(1-\frac{1}{t^2}\right)+1-\frac{1}{t}-\frac{\ln t}{t+1}\right], \tag{5}$$

where $u = U/B, t = T/B, S = 4\pi a_0^2 N R^2/B^2$ ($a_0 = 0.5292$ Å, $R = 13.61$ eV) and T is the energy of incident electrons. The electron binding energy B, kinetic energy of the orbital, U, and orbital occupation number, N, were obtained for the ground state of the target molecule with the Hartree–Fock method using the GAUSSIAN code [31], and Gaussian 6-311G+ basis set. Because the valence orbital energies obtained in this way usually differ slightly from experimental ones, we performed also the outer valence Green function calculations of correlated electron affinities and ionization potentials [32] with the GAUSSIAN code [31]. The total cross section for electron-impact ionization (ICS) is then obtained as the sum of σ^{BEB} for all molecular orbitals.

This way ICSs and ECSs have been calculated for series of boron-containing BX_3 (X = F, Cl and CH_3) molecules; results for $B(CH_3)_3$ are shown in figure 2 and listed in table 2. To compare our computational results with the experimental total cross sections (TCSs), we have finally summed the calculated ECSs and ICSs at respective energies (see figures 2 and 3).

3. Results and discussion

3.1. Trimethylborane-d_9; $B(CD_3)_3$, TMB-d_9

Figure 1 shows the energy dependence of the absolute electron-scattering total cross section for trimethylborane-d_9 measured in this work over the incident energy range from 0.4 to 370 eV. In table 1 the numerical e^-–$B(CD_3)_3$ TCS data from the present experiment are also set out for the completeness.

Over the energy range examined, the TCS function is dominated by a prominent, very broad and highly asymmetric enhancement peaking between 5 and 10 eV. At the lowest energies

Table 1. Absolute electron-scattering total cross sections for $B(CD_3)_3$ molecules; in units of 10^{-20} m^2.

E (eV)	TCS	E (eV)	TCS	E (eV)	TCS
0.4	24.3	5.5	58.2	35	46.2
0.6	25.1	6.0	59.6	40	44.4
0.8	25.5	6.5	60.6	45	42.4
1.0	25.9	7.0	61.3	50	40.5
1.2	26.0	7.5	61.4	60	38.1
1.4	25.8	8.0	60.6	70	35.6
1.6	26.8	8.5	61.2	80	33.5
1.8	27.8	9.0	61.0	90	31.4
2.0	28.9	9.5	60.0	100	30.1
2.3	31.4	10.0	59.0	110	28.1
2.5	33.4	10.5	58.2	120	26.8
2.7	35.6	11	57.0	140	24.6
3.0	38.8	12	55.6	160	22.2
3.2	41.8	14	54.2	180	20.7
3.3	43.7	16	53.3	200	19.4
3.4	45.3	18	52.4	220	18.3
3.5	44.3	20	52.0	250	16.6
3.6	45.1	22	51.4	270	16.0
3.7	45.7	25	50.5	300	14.9
4.0	48.6	27	49.4	350	13.3
4.5	52.2	30	48.0	370	12.6
5.0	55.6				

used, below 1.4 eV, the TCS appears to be nearly constant. Starting from 1.4 eV the TCS increases rapidly with energy from almost 26×10^{-20} m^2 up to slightly above 61×10^{-20} m^2 at 7 eV. Above 9 eV the TCS decreases with the energy increase. However, while up to about 12 eV the slope of the TCS curve is quite distinct, between 12 and 30 eV it becomes less steep until above 30 eV the decline increases again. At 370 eV the TCS falls slightly below 13×10^{-20} m^2.

More attentive inspection of the measured e^-–TMB-d_9 TCS energy curve reveals some supplementary, although less conspicuous features. The magnitude of these features is rather small, but they are experimentally repetitious. For instance, merely distinguishable is a very weak hump near 1.2 eV. Slightly more visible is a small narrow ($\Delta E \sim 0.2$ eV) structure located around 3.4 eV, on the steep low-energy slope of the TCS enhancement (see also inset (a) in figure 1). Two weak humps are also discernible on the ridge of the TCS enhancement, with the maxima located within 7–7.5 and 8.5–9 eV, respectively (cf inset (b) in figure 1). It is worth noting that also the dip located at 8 eV and separating the maxima was clearly distinguishable in all series of measurements. Moreover, between 14 and 27 eV a broad shoulder in the TCS curve is perceptible.

Interpretation of the aforementioned TCS features is not straightforward as neither low-energy electron-scattering intensities measured or calculated for $B(CD_3)_3$ molecule nor for its isotopic derivative, $B(CH_3)_3$, are available as yet in the literature. However, based on suggestions resulting from the comparison of the present e^-–$B(CD_3)_3$ TCS with the cross section data reported for polyatomic molecules of similar conformation (e.g. BF_3 and BCl_3) and/or with similar constituents, one may come to the conclusion that all these TCS features are resonant in origin. (i) The small hump around 1.2 eV may be related to the temporary trapping of the impinging electron in the lowest unoccupied orbital of the target molecule (our

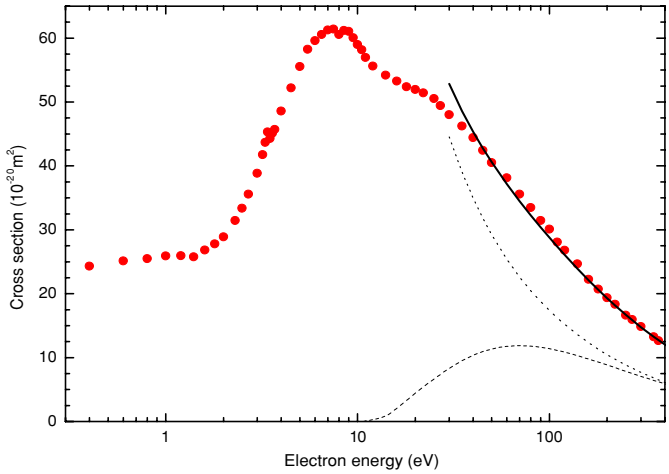

Figure 2. Present cross sections for electron scattering from TMB molecules. Experimental, $B(CD_3)_3$: (●) TCS; calculated, $B(CH_3)_3$: (· · · · · ·) ECS; (- - - -) ICS; (——) sum of ECS and ICS.

calculations localize it close to 1.2 eV) with the formation of a transient negative ion. The contribution to the TCS may come from the dissociation and/or autodetachment channels of the anion decay. Both resonant channels have been observed below 1 eV in the experiments and calculations for BCl_3 (see [1]); (ii) the small peak centred at 3.4 eV is located in the same energy range where prominent enhancement in BF_3 and the less distinct structure in BCl_3 cross sections are visible (cf figure 3). The 3–4 eV features for BF_3 and BCl_3 molecules, of geometry similar to $B(CD_3)_3$ (figure 4), have been related to resonant scattering [33, 34] leading to out-of-plane deformation and stretching of these molecules; (iii) some support for the resonant character of the broad two-peaked bump in the TCS located between 5 and 12 eV comes from the work of Murphy and Beauchamp [13]. They reported that between 6 and 14 eV the electron–$B(CH_3)_3$ scattering leads to $(CH_3)_2B{=}CH_2^-$ anion formation, in significant abundance, peaking near 10 eV. Furthermore, electron-scattering investigations for molecules with CH_2 and CH_3 groups indicate that the resonances in the vicinity of 5–7 eV and 8–10 eV are associated with the C–H bond, as temporary attachment of the incident electron in an antibonding C–H orbital [35–37]; (iv) the shoulder visible in the TCS at higher energies, may be a result of overlapping resonances between 14 and 30 eV.

The intermediate-energy part of the measured TCS for $B(CD_3)_3$ is nicely reproduced with the sum of integral elastic (ECS) and ionization (ICS) cross sections (cf figure 2) calculated within the independent atom and the binary-encounter-Bethe methods, respectively. Note that calculations were performed for $B(CH_3)_3$ even though experiment was carried out for its deuterated analogue. The difference between the TCS and the sum of ECS and ICS, clearly visible below 40 eV, results mainly from inadequacy of the IAM approximation at low energies. It is also worth noting that above 300 eV ECS and ICS are almost equal to each other. The experimental TCS at intermediate energies behaves like E^{-a} ($a \simeq 0.5$), which means that for higher energies the TCS is nearly proportional to the time the incident electron needs to cover the distance equivalent to the dimension of the target molecule.

3.2. Comparison of TCSs for boron-containing molecules: BX_3 ($X = F, Cl, CD_3$)

In figure 3 are summarized TCS measurements for the series of boron-containing molecules: BF_3 [5], BCl_3 [6] and $B(CD_3)_3$. BF_3 and BCl_3 are trigonal-planar molecules like the BC_3

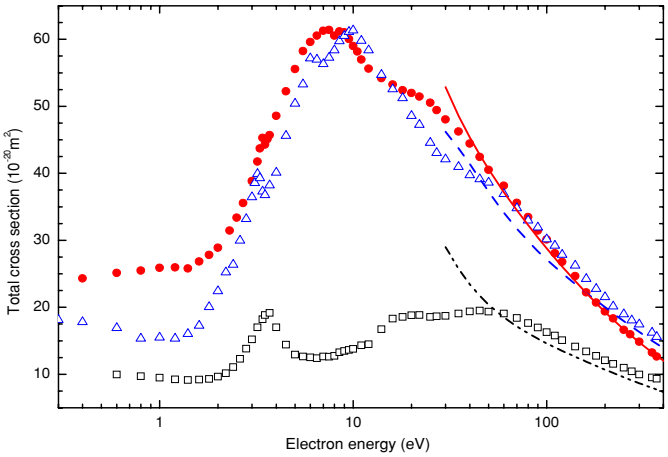

Figure 3. Comparison of total cross sections for electron scattering from boron-containing molecules. Experimental absolute TCS: (□) BF_3, [5]; (△) BCl_3, [6]; (●) $B(CD_3)_3$, present. Calculated (ECS+ICS), present: (— · · —) BF_3; (- - - -) BCl_3; (——) $B(CH_3)_3$.

Table 2. Ionization (ICS) and integral elastic (ECS) cross sections calculated for electron impact on $B(CH_3)_3$ molecules; in units of 10^{-20} m^2.

E (eV)	ICS	*E* (eV)	ICS	ECS	*E* (eV)	ICS	ECS
10.71	0.00	30	8.32	44.5	250	7.86	8.84
11	0.0613	35	9.53	39.0	300	7.08	7.68
11.5	0.173	40	10.4	35.0	350	6.44	6.81
12	0.287	45	11.0	31.8	400	5.91	6.12
12.5	0.402	50	11.4	29.3	450	5.47	5.57
13	0.517	60	11.8	25.4	500	5.09	5.10
13.5	0.669	70	11.9	22.6	600	4.48	4.39
14	0.887	80	11.8	20.5	700	4.00	3.85
15	1.42	90	11.6	18.8	800	3.63	3.44
16	2.06	100	11.4	17.4	900	3.32	3.11
17	2.70	110	11.1	16.2	1000	3.06	2.84
18	3.31	120	10.9	15.2	1200	2.66	2.43
19	3.89	140	10.3	13.6	1400	2.35	2.13
20	4.43	160	9.79	12.3	1600	2.11	1.91
22	5.41	180	9.30	11.3	1800	1.92	1.75
25	6.64	200	8.84	10.5	2000	1.76	1.62
27	7.37	220	8.42	9.74	3000	1.26	1.38

skeleton of $B(CD_3)_3$ (see figure 4). The presence of the central boron atom in each investigated molecule reflects in the feature located between 3 and 4 eV. The distinctiveness of this feature clearly decreases going from BF_3 to $B(CD_3)_3$. Whereas for BF_3 the pronounced resonant-like enhancement is located around 3.6 eV, for BCl_3 it reduces to a less distinct maximum, peaking at 3.2 eV, superimposed on the rising slope of the TCS function, and to a barely visible peak centred at 3.4 eV for $B(CD_3)_3$. Such variation of the peak magnitude across the series of the compared targets can be explained in terms of the screening of the central atom—boron—by the surrounding atoms. The screening effect increases when going from relatively small fluorine atoms to much larger chlorine ones and to the methyl groups, CD_3.

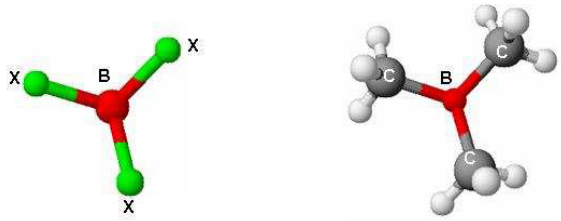

Figure 4. Schematic diagram of the ground-state BX_3 (X = F, Cl, CD_3) molecular geometry: BF_3 and BCl_3 (left); $B(CD_3)_3$ (right).

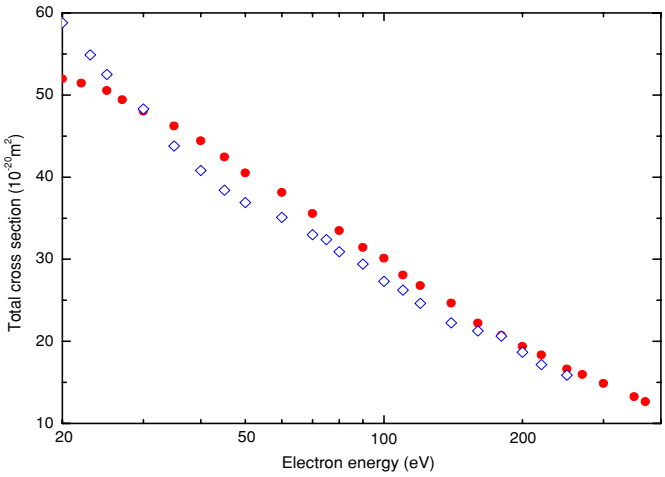

Figure 5. Comparison of the present experimental electron-scattering TCS for $B(CD_3)_3$ (●) with the tripled TCS for CH_4 (◇) [39].

At intermediate energies the experimental TCS data for BX_3 targets are compared with sums of integral elastic and ionization cross sections calculated for each molecule (see figure 3). Regarding the calculations performed, reasonable agreement was found between experimental and computational results. The most distinct difference (up to 30%) is visible for the smallest BF_3 molecule, and can be partly related to underestimation of the ionization cross section for this perfluoride. Above 200 eV the ratios of TCS values for BCl_3 [6] and for $B(CD_3)_3$ with respect to the BF_3 [5] data are nearly equal to the appropriate relation of their molecular geometrical size [8, 38].

Finally, considering the intermediate-energy e^-–$B(CD_3)_3$ total cross section, it is worth noting that in this energy range the TCS could be estimated based on data for a simpler target, CD_4. Within a crude approximation, the $B(CD_3)_3$ molecule is similar to a hypothetical molecule composed of three subunits—deuterated methane (CD_4) molecules. The carbon atom together with one deuterium of each subunit are placed in-plane; the three other deuterium atoms mimic the central B atom of the $B(CD_3)_3$ molecule. Figure 5 compares the measured cross section for e^-–$B(CD_3)_3$ with the tripled TCS data for e^-–CH_4 scattering, taken also in our laboratory [39]; we use the TCS for CH_4 because the absolute results for CD_4 are not available in the intermediate energy-range and the isotopic effect plays a minor role in the electron–molecule scattering [40–42]. Above 60 eV, the agreement between values estimated

this way and measured TCSs for $B(CD_3)_3$ is surprisingly good (the difference does not exceed 10%), which suggests that at intermediate energies the electron impact TCS for complex molecules might be roughly evaluated using the additivity rule for molecular sub-units.

4. Concluding remarks

In this work, we reported experimental absolute total cross sections for electron scattering from $B(CD_3)_3$ obtained in the 0.4–370 eV incident energy range along with intermediate-energy calculations of the integral elastic and ionization cross sections. Apart from the very pronounced TCS enhancement that peaks between 5 and 10 eV, some weak resonant-like features in the low-energy TCS function are discernible. These features may serve as a base reference for more directed studies on e^-–$B(CD_3)_3$ scattering. At intermediate energies the sum of both calculated cross sections is in good agreement with our experimental TCS results. This is also valid for BF_3 and BCl_3 molecules. Some similarities with the cross sections for boron-containing BX_3 molecules (B = F, Cl, CD_3) are also discussed.

Acknowledgments

This work was partially supported by the Polish Ministry of Education and Science (MSzWiN). Numerical calculations have been performed at the Academic Computer Center in Gdańsk (TASK).

References

[1] Christophorou L G and Olthoff J K 2004 *Fundamental Electron Interactions with Plasma Processing Gases* (New York: Kluwer)
[2] Sanche L 2005 *Eur. Phys. J.* D **35** 367–90
[3] Szmytkowski Cz and Ptasińska-Denga E 2001 *Vacuum* **63** 545–8
[4] Szmytkowski Cz and Kwitnewski S 2003 *J. Phys. B: At. Mol. Opt. Phys.* **36** 2129–38, 4865–73
[5] Szmytkowski Cz, Piotrowicz M, Domaracka A, Kłosowski Ł, Ptasińska-Denga E and Kasperski G 2004 *J. Chem. Phys.* **121** 1790–5
[6] Domaracka A, Ptasińska-Denga E and Szmytkowski Cz 2005 *Phys. Rev.* A **71** 052711
[7] Lévy H A and Brockway L O 1937 *J. Am. Chem. Soc.* **59** 2083–92
[8] Bartell L S and Carroll B L 1965 *J. Chem. Phys.* **42** 3076–8
[9] Law R W and Margrave J L 1956 *J. Chem. Phys.* **25** 1086–7
[10] Tollin B C, Schaeffer R and Svec H J 1957 *J. Inorg. Nucl. Chem.* **4** 273–8
[11] Lehmann W J, Wilson C O Jr and Shapiro I 1959 *J. Inorg. Nucl. Chem.* **11** 91–103
[12] Glockling F and Strafford R G 1971 *J. Chem. Soc.* A 1761–3
[13] Murphy M K and Beauchamp J L 1976 *J. Am. Chem. Soc.* **98** 1433–40
[14] Kappes M M, Uppal J S and Staley R H 1982 *Organometallics* **1** 1303–7
[15] Ross G S, Enagonio D, Hewitt C A and Glasgow A R 1962 *J. Res. NBS* A **66** 59–63
[16] Jiang X, Au F C K and Lee S T 2002 *J. Appl. Phys.* **92** 2880–3
[17] Kupich M, Grunsky D, Kumar P and Schröder B 2004 *Sol. Energy Mater. Sol. Cells* **81** 141–6
[18] Bederson B and Kieffer L J 1971 *Rev. Mod. Phys.* **43** 601–40
[19] Szmytkowski Cz and Możejko P 2001 *Vacuum* **63** 549–54
[20] Szmytkowski Cz, Maciąg K and Karwasz G P 1996 *Phys. Scr.* **54** 271–80
[21] Knudsen M 1910 *Ann. Phys. Lpz.* **31** 205–29
[22] Nelson R N and Colgate S O 1973 *Phys. Rev.* A **8** 3045–9
[23] Szmytkowski Cz, Możejko P and Kasperski G 1997 *J. Phys. B: At. Mol. Opt. Phys.* **30** 4363–72
[24] Możejko P, Żywicka-Możejko B and Szmytkowski Cz 2002 *Nucl. Instrum. Methods Phys. Res.* B **196** 245–52
[25] Możejko P and Sanche L 2003 *Radiat. Environ. Biophys.* **42** 201–11
[26] Mott N F and Massey H S W 1965 *The Theory of Atomic Collisions* (Oxford: Oxford University Press)
[27] Joshipura K N and Vinodkumar M 1997 *Z. Phys.* D **41** 133–7

[28] Salvat F, Martinez J D, Mayol R and Parellada J 1987 *Phys. Rev.* A **36** 467–74
[29] Padial N T and Norcross D W 1984 *Phys. Rev.* A **29** 1742–8
[30] Hwang W, Kim Y K and Rudd M E 1996 *J. Chem. Phys.* **104** 2956–66
[31] Frisch M J *et al* 2003 *GAUSSIAN 03*, Revision B.05 (Pittsburgh: Gaussian)
[32] Zakrzewski V G and von Niessen W 1994 *J. Comput. Chem.* **14** 13–8
[33] Tronc M, Malegat L, Azria R and Le Coat Y 1982 *J. Phys. B: At. Mol. Phys.* **15** L253–8
[34] Tossell J A, Moore J H and Olthoff J K 1986 *Int. J. Quantum Chem.* **29** 1117–26
[35] Boesten L, Tanaka H, Kubo M, Sato H, Kimura M, Dillon M A and Spence D 1990 *J. Phys. B: At. Mol. Opt. Phys.* **23** 1905–14
[36] Allan M and Andric L 1996 *J. Chem. Phys.* **105** 3559–68
[37] Możejko P, Ptasińska-Denga E, Domaracka A and Szmytkowski Cz 2006 *Phys. Rev.* A **74** 012708
[38] Lide D R 1995–1996 *CRC Handbook of Chemistry and Physics* 76th edn (Boca Raton, FL: CRC Press)
[39] Zecca A, Karwasz G, Brusa R S and Szmytkowski Cz 1991 *J. Phys. B: At. Mol. Opt. Phys.* **24** 2747–54
[40] Schram B L, van der Wiel M J, de Heer F J and Moustafa H R 1966 *J. Chem. Phys.* **44** 49–54
[41] Tice T and Kivelson D 1967 *J. Chem. Phys.* **46** 4743–7
[42] Szmytkowski Cz, Maciąg K, Koenig P, Zecca A, Oss S and Grisenti R 1991 *Chem. Phys. Lett.* **179** 114–8